Physiologically-Based Pharmacokinetic Modeling in Renal and Hepatic Impairment Populations: A Pharmaceutical Industry Perspective

Tycho Heimbach[1,*,†], Yuan Chen[2], Jun Chen[3], Vaishali Dixit[4,†], Neil Parrott[5], Sheila Annie Peters[6], Italo Poggesi[7], Pradeep Sharma[8], Jan Snoeys[9], Mohamad Shebley[10], Guoying Tai[11], Susanna Tse[12], Vijay V. Upreti[13], Ying-Hong Wang[14,‡], Alice Tsai[15], Binfeng Xia[16], Ming Zheng[17], Andy Z.X. Zhu[18] and Stephen Hall[19]

The predictive performance of physiologically-based pharmacokinetics (PBPK) models for pharmacokinetics (PK) in renal impairment (RI) and hepatic impairment (HI) populations was evaluated using clinical data from 29 compounds with 106 organ impairment study arms were collected from 19 member companies of the International Consortium for Innovation and Quality in Pharmaceutical Development. Fifty RI and 56 HI study arms with varying degrees of organ insufficiency along with control populations were evaluated. For RI, the area under the curve (AUC) ratios of RI to healthy control were predicted within twofold of the observed ratios for > 90% (*N* = 47/50 arms). For HI, > 70% (*N* = 43/56 arms) of the hepatically impaired to healthy control AUC ratios were predicted within twofold. Inaccuracies, typically overestimation of AUC ratios, occurred more in moderate and severe HI. PBPK predictions can help determine the need and timing of organ impairment study. It may be suitable for predicting the impact of RI on PK of drugs predominantly cleared by metabolism with varying contribution of renal clearance. PBPK modeling may be used to support mild impairment study waivers or clinical study design.

Physiologically-based pharmacokinetic (PBPK) modeling has seen significant applications in model-informed drug discovery and development over the past years.[1] When mechanistic PBPK models have been verified and validated, they can be used to extrapolate or to predict pharmacokinetic (PK) changes with confidence beyond the studied scenarios or to aid in risk assessments.[2] Consequently, recommendations for concomitant medications and dose adjustment in specific populations have been approved based on PBPK modeling in lieu of clinical studies in a growing number of drug labels over the past several years.[3,4]

Currently, the majority of PBPK applications involve predictions of drug–drug interactions (DDIs), mainly mediated via inhibition or induction of cytochrome P450 (CYP) enzymes and, to a lesser extent, uridine diphosphate glucuronosyl transferases (UGTs) and transporters. For example, 60% of the 254 PBPK submission records to the US Food and Drug Administration (FDA) from 2008 to 2017 were for DDI predictions[5,6] (Grimstein *et al*., 2019). Similar percentages were reported by the European Medicines Agency (EMA)[7] and the Japan Pharmaceuticals and Medical Devices Agency (PMDA).[8] Successful application of PBPK modeling to specific (e.g., pediatrics and geriatrics) or diseased (e.g., organ impaired) populations requires a good understanding of the physiological and biological changes that can impact drug disposition in these populations compared with healthy control subjects.

Both renal and hepatic impairments are associated with multiple pathophysiological and biological changes. Renal impairment

[1]Pharmaceutical Sciences, Merck & Co., Inc, Rahway, New Jersey, USA; [2]Department of Drug Metabolism and Pharmacokinetics, Genentech, Inc, South San Francisco, California, USA; [3]Clinical Pharmacology, Alkermes Inc, Waltham, Massachusetts, USA; [4]Drug Metabolism and Pharmacokinetics, Kymera Therapeutics, Watertown, Massachusetts, USA; [5]Pharmaceutical Sciences, Roche Innovation Center Basel, F. Hoffmann-La Roche Ltd, Basel, Switzerland; [6]Translational Medicine, Merck Healthcare KGaA, Darmstadt, Germany; [7]Clinical Pharmacology and Pharmacometrics, Janssen, Milan, Italy; [8]Clinical Pharmacology & Quantitative Pharmacology, Clinical Pharmacology & Safety Sciences, R&D, AstraZeneca, Cambridge, UK; [9]Department of Drug Metabolism and Pharmacokinetics, Janssen R&D, Beerse, Belgium; [10]Clinical Pharmacology and Pharmacometrics, AbbVie Inc, North Chicago, Illinois, USA; [11]Department of Drug Metabolism and Pharmacokinetics, GlaxoSmithKline Plc, Collegeville, Pennsylvania, USA; [12]Department of Pharmacokinetics, Dynamics and Metabolism, Pfizer Inc, Groton, Connecticut, USA; [13]Clinical Pharmacology, Modeling & Simulation, Amgen Inc, South San Francisco, California, USA; [14]Department of Pharmacokinetics, Pharmacodynamics, and Drug Metabolism, Merck & Co, Inc, Kenilworth, New Jersey, USA; [15]Department of Drug Metabolism and Pharmacokinetics, Vertex Pharmaceuticals Inc, Boston, Massachusetts, USA; [16]PK/PD Group, Pharmacokinetics, Dynamics and Metabolism, Sanofi, Bridgewater, New Jersey, USA; [17]Clinical Pharmacology and Pharmacometrics, Bristol-Myers Squibb, Princeton, New Jersey, USA; [18]Drug Metabolism and Pharmacokinetics, Takeda Pharmaceuticals International, Co, Cambridge, Massachusetts, USA; [19]Department of Drug Disposition, Lilly, Indianapolis, Indiana, USA. *Correspondence: Tycho Heimbach (Tycho.Heimbach@Merck.com)

[†]Formerly at Novartis (T.H.) and Formerly at Eisai Inc (V.D.).
[‡]The author was an employee of Merck at the time this work was conducted.

Received June 23, 2020; accepted November 17, 2020. doi:10.1002/cpt.2125

is characterized by reduced glomerular filtration and/or tubular secretion, and accumulation of uremic toxins resulting from the loss of renal function, as well as hypoalbuminemia in some patients. Uremic toxins down-regulate the expression of CYP enzymes and may also directly inhibit CYP-mediated metabolism.[9] Uremic solutes are also known to inhibit renal organic anion transporters (OATs).[10] Renal insufficiency is also expected to increase α-acidic glycoprotein (AAG), reduce hematocrit, and reduce the gastric emptying rate. Pathophysiological changes can decrease the clearance of drugs that are primarily eliminated by metabolic as well as renal pathways.

Liver impairment may be caused by multiple chronic disease conditions which destroy the liver parenchyma, ultimately leading to hepatic and biliary cirrhosis. Liver cirrhosis is characterized by a progressive decline in hepatic blood flow, hematocrit, alpha-1-glycoprotein (AGP), albumin, functional hepatocytes, and biliary excretion. Moreover, there are alterations in expression and activity of hepatic transporters[11] and metabolizing enzymes as well as reduced duodenal CYP3A expression and activity.[12] In cirrhotic patients, the formation of concomitant connective tissue and nodules in the liver can lead to hepatic venous outflow obstruction,[13] leading to increased intrahepatic vascular resistance and sinusoidal pressure. This can trigger the insertion of a side-to-side porto-caval shunt, which relieves the sinusoidal pressure.[14] However, with disease progression, the compensatory mechanism of porto-caval shunt becomes inadequate and splanchnic and peripheral flow are altered. The resulting reduction in the effective arterial blood volume leads to a diminished renal blood flow in cirrhotic patients, which in turn stimulates the renin-angiotensin-aldosterone system, sympathetic nervous system, and antidiuretic hormone resulting in renal artery vasoconstriction, sodium retention, volume expansion, and increased cardiac output (hyperdynamic circulation). Eventually, these changes lead to a hepatorenal syndrome or acute renal failure with a low glomerular filtration rate (GFR).

Because the liver, intestine, and kidney are the major sites for metabolism and elimination, the morphological and physiological changes in these organs can significantly impact the PK of a drug and/or its active metabolites.[15] To ensure adequate efficacy and safety, regulatory agencies recommend conducting a PK study for drugs of narrow therapeutic index that are predominantly eliminated (> 50%) by the impaired organ when they are likely to be used by subjects with different levels of impairment.[16–19] Disease severity was classified based on the estimated GFR and albuminuria for renal impairment and on Child-Pugh (CP) classification comprising classes A (mild), B (moderate), and C (severe) for hepatic impairment.[20] Based on the study results, dose adjustments may be recommended in the label. It is noteworthy however, that the CP classification has not been designed to estimate the impact of hepatic impairment on the absorption, distribution, metabolism, and excretion (ADME) of various drugs. Accurate staging of hepatic insufficiency would require a variety of imaging and noninvasive biomarkers for the multiple mechanisms leading to liver insufficiency.[21]

However, hepatic and renal impairment studies are resource intensive and it can take several years to recruit enough patients with different levels of disease severity.[22] For example, for crizotinib it took more than 4 years to complete the hepatic impairment study due to recruitment challenges.[23] PBPK models are ideally suited to incorporate the multitude of pathophysiological changes in organ impairment[14,24,25] and to predict the combined impact of disease and other covariates on the exposure of drugs that are renally or hepatically eliminated. Model simulations can supplement limited clinical data when recruitment is incomplete. Extending the insight gained from studies that have poor representation of some patient subsets can be particularly useful in oncology settings as well as in pediatric applications.[26]

In this present research, the predictive performance of PBPK models for hepatic and renal impairment populations was evaluated using clinical trial data contributed by 19 member companies in a working group under the Translational and ADME Sciences Leadership Group (TALG) and the Clinical Pharmacology Leadership Group (CPLG) of the International Consortium for Innovation and Quality in Pharmaceutical Development (IQ Consortium). Relatively few examples of PBPK predictions in renally and hepatically impaired patients have been published to date (**Table S1a,b**). They involved a small number of compounds and did not follow a standardized workflow, making it difficult to draw firm conclusions on the predictive performance. The objectives of this IQ PBPK Organ Impairment Working Group were therefore to (i) collect a large set of data and use a consistent approach to evaluate the accuracy of the predictions, (ii) investigate the potential mechanisms in cases where the predictions were not accurate, and (iii) provide recommendations on the application of PBPK predictions to design drug development strategies in renally and hepatically impaired populations.

APPROACH OF PBPK MODELING FOR RENAL AND HEPATIC IMPAIRMENT POPULATIONS

To avoid selection bias, all compounds from the 19 member companies with organ impairment studies and with comprehensive PK data sets were included in this study. There were in total 29 compounds with 106 organ impairment study arms. Key ADME compound information and known biotransformation pathways have been summarized in **Table 1**. The majority of compounds in the data set were eliminated predominantly via metabolism, with varying contribution (0–50%) of renal clearance. A summary of demographic data and study design of the clinical renal and hepatic organ impairment data can be found for most compounds in **Tables S2 and S3**, respectively. Human ADME study data were available for model development for nearly all compounds (19 out of 25 for compounds with RI assessment and 21 out of 27 for compounds with HI assessment; ~ 75% in either case (**Tables S7a,b** and **S8a,b**). In a few cases detailed study data were not available. For a few compounds, e.g., H626T, Q679L, T535Q, Y582A, only HI data were available (**Table S8a,b**).

For renal impairment assessments, clinical data were included from 25 compounds. A total of 50 study arms included 8 in mild, 14 in moderate, 25 in severe renal impairment, and 3 in end-stage renal disease (ESRD). For hepatic impairment assessments, data from 27 compounds with a total of 56 study arms were available. Included were 18 study arms in patients with mild hepatic

Table 1 Summary of ADME properties for compounds collected by the IQ working group

Compound	Fu	CL_{iv} (L/h)	% CL_r	% $CL_{-biliary}$	Biotransformation
A242N	0.3	41 (HV) 33(Pat)	3.5 (Pat)		72% CYP3A, 18% FMO3, 3.5% renal, 3.5–6.5% others
B222R	0.005	3.07			70% CYP3A4; 30% CYP2C19
B785F	0.07	14.75 (po)	7.3		57% CYP1A2, 27% UGT, 8.4% CYP2C8
B994T	0.67	42	38		25% CYP3A, 37% other non-CYP enzymes
C213X	0.495p	8.12p	15	43	42% metabolism via demethylation, oxidation, and glutathione conjugation
D268Y	0.013	30.6	0		85% CYP2D6, 15% CYP1A2
D384S	0.006	4.24	11	31	56% CYP3A
D863C	0.61	24.7	29		54% CYP3A, 17% CYP2C19
E929K	0.09	41.4			20% CYP2D6, 80% CYP1A2
H626T	0.00814		< 0.01	15	85% non-CYP enzymes; 15% unknown enzymes
H938P	0.007	1.34 (po)	< 0.8		15% CYP3A4, 85%UGT1A1
J269A	0.24	3.73	10		90% CYP3A
K946A	0.091	9.6 (po)			75% CYP2D6
M731N	0.0002	3.11	0		79.2% CYP2C9, 18.6% CYP3A, 2.2% other metabolites
N314T	0.42	14.80	6		80% CYP1A2
N929A	0.85p	23.1	25	75	Negligible metabolism; substrates of hepatic uptake or efflux transporter
P662Y	0.02	4.06 (po)			> 90% CYP3A
Q679L	0.04–0.20	38.6 (po)	0.5		70% CYP, > 20% others
Q731V	0.7	21.1	45		10% CYP3A, 25% UGT, ~ 20% other (undefined)
S471Q	0.025	9	0	0	75% CYP3A4 oxidation, 25% amide hydrolysis and N-dearylation
S537Y	0.025	0.8	16	16	68% CYP3A
S961T	0.204	1420 (po)	6.5		40% CYP3A, 60% CYP2D6 (*in vitro*)
T535Q	0.2	47.2 (po)			40% CYP3A, 60% CYP2C9 and others (OATP uptake)
T631W	0.041	27.7	2		95% CYP3A
T765J	0.403		53		28% hepatic; 19% hydrolysis
U924W	0.063		1–2		17% AO, 27% CYP3A, 23% nonenzymatic
V597G	0.104		14	0	39% CYP3A, 10% CYP2D6, 3% CYP2C19, 34% other
Y276D	0.0241	32.2 (po)	6	5	79% CYP3A, 6% CYP2C19, 4% CYP2D6 (*in vitro*)
Y582A	0.0326	61.2			96% CYP3A

ADME, absorption, distribution, metabolism, and excretion; $CL_{biliary}$, biliary clearance; CL_{iv}, plasma clearance after IV administration of the drug; CL_r, renal clearance; CYP, cytochrome P450; FMO3, Flavin-containing monooxygenase 3; Fu, free fraction in plasma protein; HV, healthy volunteer; IQ, International Consortium for Innovation and Quality in Pharmaceutical Development; OATP, organic anion transporting polypeptide; Pat, patient; po, oral administration; UGT, uridine diphosphate-glucuronosyltransferase.

impairment, 25 study arms with moderate hepatic impairment, and 13 study arms with severe hepatic impairment.

PBPK model development strategy and model verification

A general PBPK modeling strategy workflow is depicted in **Figure 1**. PBPK models for all compounds were constructed by modelers from the contributing companies using the population-based ADME simulator (Simcyp V15, Certara, Sheffield, UK). Other commercial PBPK platforms (e.g., GastroPlus) and open PBPK modeling platforms (e.g., PK-Sim, Simbiology, Monolix, Berkeley-Madonna, etc.) are available to use for organ-impaired population PK predictions. The performance of the PBPK models was validated by the contributing companies by simulating relevant clinical trials such as single ascending dose and multiple ascending dose, or DDI studies in either healthy volunteers or patients. While this IQ white paper does not intend to recommend specifics about model verification, such as to provide recommendations for parameter sensitivity analyses, the selection of parameters and associate ranges for the analyses should be based on the specific ADME properties of the study compounds, particularly the pathologic factors that can significantly impact the variability in renal and hepatic impairment populations, such as metabolic enzyme expression level and plasma protein binding.[27,28] When applying the PBPK model in HI/RI patients for a DDI prediction, the degree of induction and inhibition can be impacted by the metabolic enzyme expression levels in the corresponding HI/RI patient group, and thereby, parameter sensitivity approaches to investigate their global relationships before

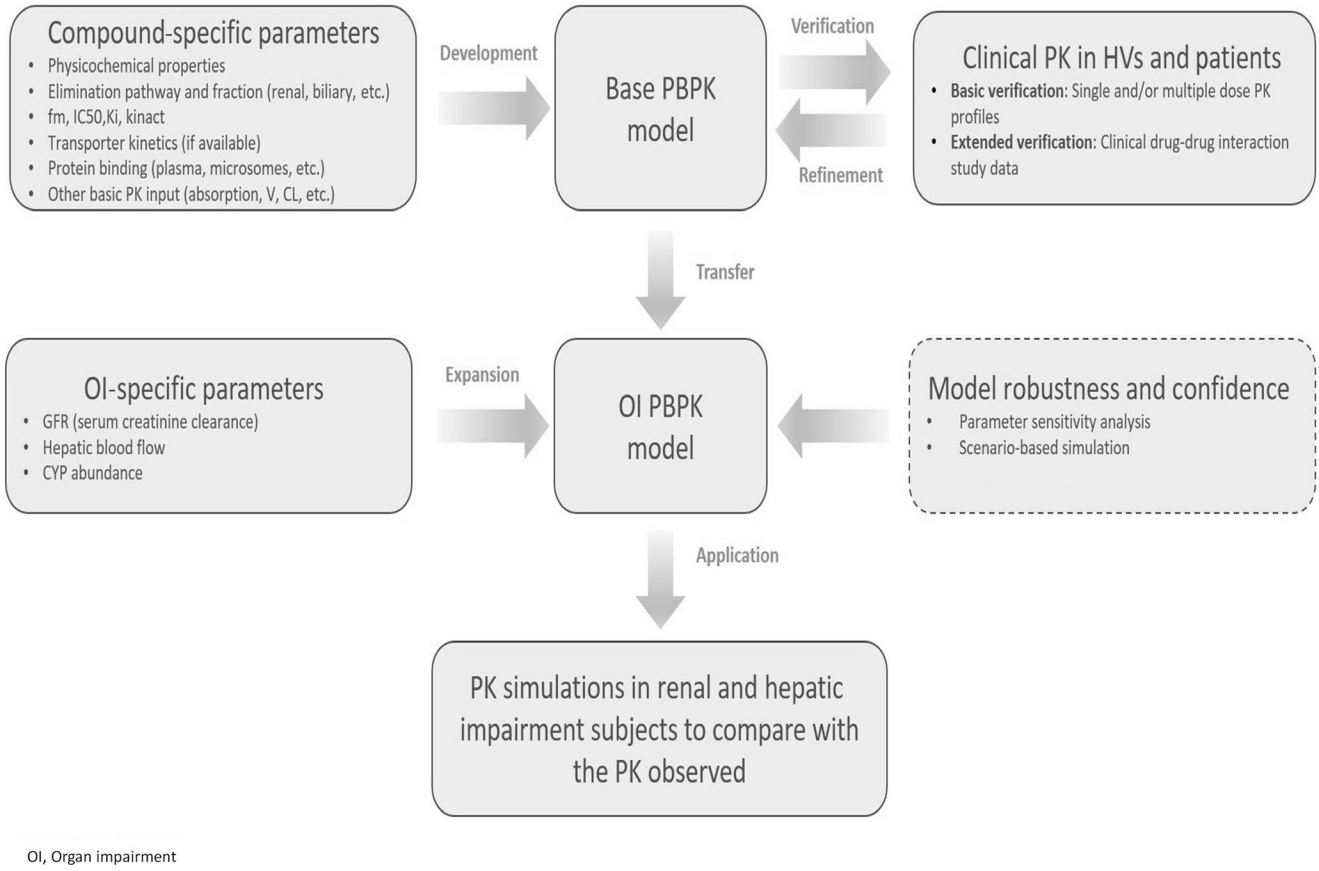

Figure 1 Schematic workflow for the development of an organ impairment PBPK model. CL, clearance; CYP, cytochrome P450; fm, fraction metabolized; GFR, glomerular filtration rate; HVs, healthy volunteers; IC_{50}, concentration of drug producing 50% inhibition; Ki, inhibitory constant; PBPK, physiologically-based pharmacokinetics; PK, pharmacokinetics; V, volume of distribution.

starting to simulate a specific study scenario.[27] In addition, the scenario-based simulation can investigate different hypothetical conditions when a modeling compound undergoes multiple metabolic or excretive pathways simultaneously (e.g., dual substrate of CYP enzymes and transporters) or key input parameters were not certain when performing the simulation.[28] Such an approach can typically provide more useful insights in optimization of PBPK models when modelers have to evaluate the risk of study outcome by understanding the "worst-case" scenario."

The predicted PK parameters and PK profiles were generated using similar study design and compared with the observed clinical data to ensure that the models adequately described the PK of the corresponding compounds. To further establish confidence in model robustness, assignment of clearance pathways for each compound model was verified using simulations of inhibition DDI data in which the study compound is a victim drug, when DDI data were available. If a compound is metabolized by enzymes with known genetic polymorphism, simulation of the PK profiles in subjects with different metabolic status (e.g., extensive or poor metabolizers) was also performed as part of the verification. PBPK compound model files in Simcyp for probe-interacting drugs (e.g., rifampin, midazolam, ketoconazole, and itraconazole) were used for the DDI simulations.

Model evaluation was conducted in two steps. As a first step, model-predicted exposures (maximum plasma drug concentration (C_{max}) and area under the curve (AUC)) of compounds were compared for healthy subjects; this was done to ensure the predictivity of the PBPK model in a healthy population (matched healthy control subjects) ahead of predicting the organ impairment population. The criteria used for this first-step model evaluation was how many values are predicted within 25% of the observed values, how many within 50% of the observed values, and how many are predicted within twofold of the observed values. If the simulated compound exposures were within twofold for the healthy population, the compound models were considered acceptable for simulating organ impairment and the model was deemed verified in the first step.

In the second step, following verification of the compound model in predicting healthy population, simulations were performed in mild, moderate, or severe organ-impaired subjects matching the clinical study design (dose, dosing frequency) and age range of the available study cohorts. The Simcyp renal and hepatic organ impairment populations were used to simulate the pharmacokinetics in the organ-impaired groups and the Simcyp healthy volunteers (HVs) population was used for the control group with the age distribution adjusted to match that in the corresponding organ-impairment population. Ten trials with 10 subjects (100 virtual subjects) were simulated with the gender ratio of the virtual population matching the reported clinical study data or with a value of 0.5 assumed if this information was

not available. In this second step, the Guest criterion[29] was used to compare the predicted AUC ratios of organ impairment relative to control healthy populations vs. the observed AUC ratios of organ impairment relative to control healthy populations. With the Guest criterion,[29] the delta value was 1.25 and 20% CV was incorporated. With the observed AUC ratio = 1, the bounds correspond to the bioequivalence bounds (0.80–1.25). For each verified compound model, simulations were performed in mild, moderate or severe organ-impaired subjects matching the clinical study design (dose, dosing frequency) and age range of the available study cohorts. The Simcyp renal and hepatic organ impairment populations were used to simulate the pharmacokinetics in the organ impaired groups and the Simcyp HVs population was used for the control group with the age distribution adjusted to match that in the corresponding organ impairment population (**Tables S2–S5**). Typically, 10 trials with 10 subjects (i.e., 100 virtual subjects) were simulated with the gender ratio of the virtual population matching the reported clinical study data or with a value of 0.5 assumed if this information was not available.

Renal impairment population PBPK modeling

Two renal impairment populations (moderate and severe) were applied based on GFR classification (Renal GFR 30–60 and Renal GFR < 30) as defined in the Simcyp Simulator. After consultation with Simcyp/Certara Inc, a mild renal impairment population file was created by adapting the Sim-renal GFR_30–60 population by setting GFR to between 60 and 90 mL/min per 1.73 m^2, reverting the CYP abundance to that of the healthy volunteers, serum creatinine (93–102 μmol/L), gastric residence time (fasted = 0.55 hour; fed = 1.38 hour) and albumin (ratio = 0.93 to HV, male) and hematocrit (ratio = 0.92 to HV, male). The key physiological differences between healthy volunteers and patients from renal impairment populations used for this work are listed in **Table S4**. Potential inhibition of enzymes and transporters by uremic toxins is not implemented in Simcyp version 15.

Hepatic impairment population PBPK modeling

The mechanistic hepatic impairment population in Simcyp considers the demographics of liver cirrhosis patients, including the age distribution and the higher frequency in males compared with females. It implements the disease-relevant changes for three hepatically impaired subpopulations with varying levels of liver cirrhosis severity according to CP scores: 5 & 6, A (mild), 7 to 9, B (moderate), and 10 to 15, C (severe).[20] Progressive declines in hepatic blood flow, hematocrit, AGP, albumin, and CYP enzyme abundance, as well as a reduction in intestinal CYP3A4/5 expression and catalytic activity and proportionate changes to other intestinal CYP enzymes[12] have been incorporated. The model also accounts for the hepatic shunt-induced fractional changes in mesenteric blood flow, and a decrease in gastric residence time with increasing disease severity under both fasted and fed conditions is considered. The key physiological differences between healthy volunteers and patients with liver cirrhosis as implemented in Simcyp Version 15 are listed in **Table S5**.[24] The decrease in the liver size with increasing severity of cirrhosis has been derived from a meta-analysis of five studies for the different CP categories. CYP enzyme expression and activity are based on *in vitro* data.[24] However, apart from a loss functional mass leading to changes in enzyme abundances and activity, diseased livers may also have altered scalars (milligram protein per gram liver) which is not considered in Simcyp Version 15.

The predicted C_{max} and AUC in healthy subjects were first compared with the observed data to ensure model predictivity for a healthy population. Subsequently, the predicted C_{max} and AUC ratios of organ impairment relative to control healthy populations vs. the observed C_{max} and AUC ratios were plotted and assessed.

PREDICTIVE PERFORMANCE OF PBPK MODELS FOR HEPATIC AND RENAL IMPAIRMENT POPULATIONS

PBPK modeling of renal impairment

Summaries of key ADME properties of each compound are shown in **Table 1**. The patient demographic data and clinical trial design for the renal impairment trials are summarized in **Table S2**. Performance of the PBPK models was initially assessed by comparison of the predicted with observed AUC and C_{max} of the compounds in matched healthy control subjects (**Figure S1**). Seventy-six percent of AUC (19/25) and 67% of C_{max} (16/25) were predicted within 25% of the observed values. Ninety-two percent of AUC (23/25) and C_{max} (22/24) were within 50% of the observed values. All the predicted AUCs and C_{max} were within the twofold error except for one compound whose predicted AUC was approximately threefold of the observed value.

Across all clinical data sets, the observed effects of renal impairment were modest, with the maximum observed mean AUC ratio (renal impairment/control) being 1.7, 2.2, and 2.2 for mild, moderate, and severe/ESRD impairments, respectively (**Table 2**). Of the combined 50 renal impairment study arms, 88% of model-predicted effects fell within the Guest criterion, an alternative method to the common twofold criteria approach, which assesses prediction success with a variable prediction margin dependent on the particular AUC ratio.[29] AUC ratios that did not meet the Guest criterion were all in the severe renal impairment and ESRD groups (**Table 2** and **Figure 2a**), of which two cases had prediction errors greater than twofold. In both cases, decreased exposure was observed in renal impairment patients compared with healthy control groups (AUC ratio of 0.6–0.7) (**Table 2**). Similar trends were observed for the renally impaired to healthy C_{max} ratios (**Table 3**, **Figure 2b**). Prediction errors were also calculated and are shown in **Table S7a,b**.

Knowing that plasma proteins such as albumin or alpha-1 acid glycoprotein (AGP) are affected in different renal disease stages, PBPK models used *ex vivo*–measured fraction unbound in plasma values when available. A comparison of the predicted and observed fraction unbound in plasma in healthy subjects and patients renal impairment (**Figure 2c**) showed that only two cases were predicted outside the twofold line, one in the severe RI group and one in the moderate RI group. In summary, PK changes in mild and moderate RI, along with plasma protein binding changes, were well predicted by PBPK modeling, while there was a tendency to overpredict the

Table 2 Comparison of observed and predicted AUC ratio in renal impairment studies

	Mild renal impairment			Moderate renal impairment			Severe renal impairment			ESRD		
Compound	Observed	Predicted	Pred/Obs	Observed	Predicted	Pred/Obs	Observed	Predicted	Pred/Obs	Observed	Predicted	Pred/Obs
A242N	1.62	1.83	1.13	1.94	1.87	0.96	2.67	1.61	0.60			
B222R							1.22	1.38	1.13			
B785F				1.48	1.52	1.03	1.32	1.35	1.02			
B994T				1.50	1.47	1.22	1.92	1.64	0.85			
C213X				1.82	1.28	0.70	1.21	1.51	1.25			
D268Y										2.00	1.65	0.83
D384S				2.10	3.05	1.45	1.94	2.80	1.44			
D863C	1.37	1.27	0.93	1.43	1.68	1.17	2.23	2.35	1.05			
E929K										2.16	2.77	1.28
H938P							0.61	0.85	1.39			
J269A							1.43	1.54	1.1			
K946A	0.89	1.00	1.12				1.42	1.70	1.20	0.71	1.55	2.18
M731N							1.24	0.97	0.78			
N314T	1.39	1.13	0.81	1.49	2.04	1.37	1.10	1.76	1.61			
N314Tm	1.72	1.65	0.96	3.48	2.35	0.68	5.85	4.49	0.77			
N929A				1.26	1.34	1.06	1.66	1.37	0.83			
P662Y							1.13	1.19	1.06			
Q731V	1.42	1.30	0.92	1.56	1.46	0.94	2.08	1.81	0.87			
S537Y							1.60	1.30	0.81			
S961T							0.99	1.10	1.11			
T631W							0.64	1.56	2.44			
T765J				1.52	1.59	1.05	1.83	1.80	0.98			
U924W	0.90	0.95	1.05	0.90	0.85	1.05	1.21	0.74	0.61			
V597G	0.64	0.86	1.34	1.41	1.13	0.80	0.60	1.09	1.80			
Y276D				1.32	1.60	1.21	1.63	1.57	0.96			

AUC, area under the curve; ESRD, end-stage renal disease; Obs, observed; Pred, predicted.

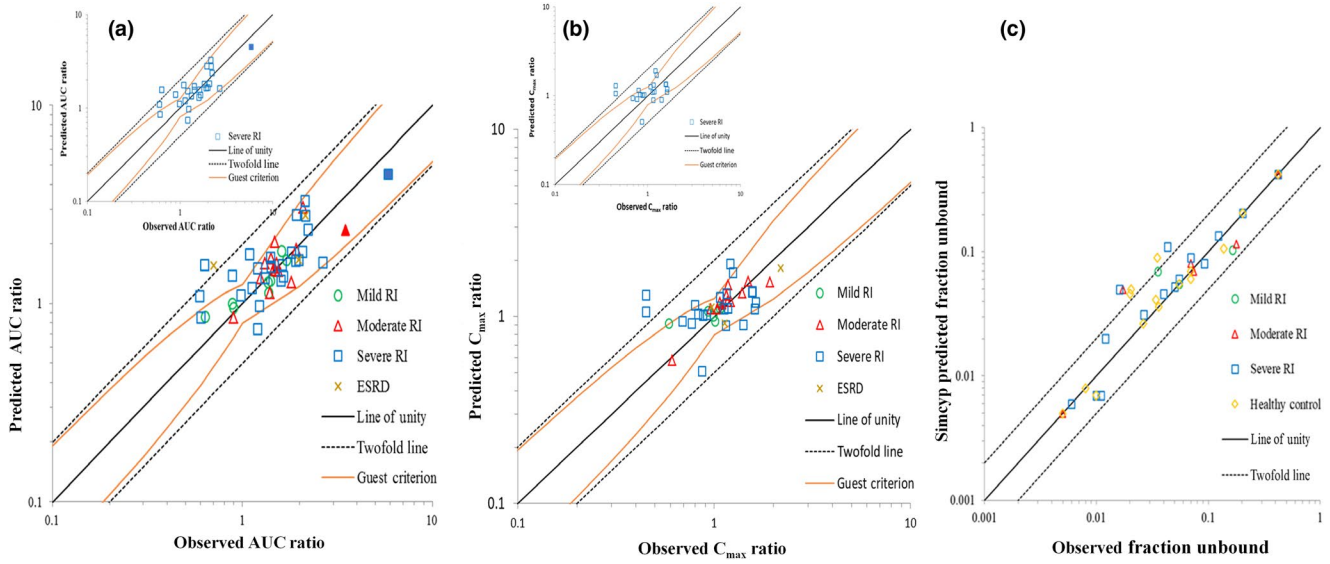

Figure 2 Renal Impairment. (**a**) Comparison of predicted with observed AUC ratios of renal impairment (RI) patients to matched healthy control subjects (*N* = 8 mild, 14 moderate, 25 severe, 3 ESRD). Solid markers represent the major metabolite of N314T. (**b**) Comparison of predicted with observed C_{max} ratios of renal impairment patients to matched healthy control subjects (*N* = 8 mild, 14 moderate, 25 severe, 3 ESRD). (**c**) Comparison of predicted with observed fraction unbound in plasma of renal impairment patients (*N* = 15 healthy, 4 mild, 6 moderate, 15 severe). AUC, area under the curve; C_{max}, maximum plasma drug concentration; ESRD, end-stage renal disease.

effect with increasing disease severity. However, it has to be noted that this data set is limited in the severe RI and ESRD categories.

PBPK modeling of hepatic impairment

Performance of the PBPK models for healthy control subjects was assessed prior to hepatic impairment modeling. A comparison of predicted with observed AUC and C_{max} of the compounds in matched healthy subjects was performed (**Figure S2**). Eighty-five percent of AUC and 76% of C_{max} were predicted within 25% of observed values. Ninety-six percent of AUC and 76% of C_{max} were within 50% of the observed values. All the predicted AUCs were within the twofold error. Prediction errors were also calculated and are shown in **Table S8a,b**.

In the clinical data sets, the observed AUC for mild hepatic impairment patients were within twofold of the healthy controls except for one compound with moderate clearance which was predominantly metabolized by CYP3A (fraction metabolized of 96%). Observed AUC ratios were between 0.6-fold and 8-fold for patients with moderate hepatic impairment, and between 0.6-fold and 9.5-fold for patients with severe hepatic impairment (**Table 4**). In most cases, the effects of hepatic impairment on drug exposure increased as the severity of disease increased (**Table 4**). Within each CP category, the fraction eliminated by a particular pathway (e.g., CYP3A) seemed not the only determinant of the impact of hepatic impairment, indicating that other factors may also play an important role. In general, low-clearance compounds (plasma clearance after intravenous administration of the drug < 20 L/h) were less affected by hepatic impairment (**Figure 3**).

The predictive performance of the hepatic impairment population models was evaluated by comparing the observed and predicted AUC ratios between patients with hepatic impairment and matched healthy subjects (**Figure 3a–c**). In general, the models tended to overpredict the effects of hepatic impairment on PK with no false-negative predictions. Among the three cirrhosis population models, the CP-A model appeared to have the best performance with only one prediction outside the twofold error range. However, when the Guest criteria[29] were applied, greater than 50% of the predictions were outside the upper limit. For the CP-B and CP-C cirrhosis models, ~ one-third of the predicted AUC ratios were outside the twofold error range (**Figure 3a–c**). The majority of compounds that fell outside the upper limit of the Guest criteria or the twofold error range had a low systemic clearance, defined here as lower than 20 L/h. The impact of hepatic impairment was reasonably predicted for compounds with systemic clearance greater than 20 L/h, with 83% of the predictions for CP-C and 82% of the predictions for CP-B within the Guest criteria, and 100% of the predictions for CP-B within twofold error range (**Figure 3**). For compounds that were studied clinically in more than one hepatic impairment category, when the effects of moderate hepatic impairment were predicted within twofold, the effects of mild or/and severe hepatic impairment were generally also predicted within twofold regardless of their clearance (**Table 4**). Similar trends were observed for the hepatic impaired to healthy C_{max} ratios (**Figure 3d–f** and **Table 5**).

LEARNINGS AND CHALLENGES

Successful application of PBPK modeling in lieu of clinical trials and in support of labeling has been demonstrated mainly in drug–drug interactions, absorption and food effect for BCS class I and II drugs, and, to some extent, pediatric dose selection. Although isolated examples for the use of PBPK modeling in the assessment of hepatic and renal organ impairment exist (**Table S1a,b**), a systematic evaluation of the predictive performance of PBPK in various stages of renal and hepatic

Table 3 Comparison of observed and predicted C_{max} ratio in renal impairment studies

	Mild Renal Impairment			Moderate Renal Impairment			Severe Renal Impairment			ESRD		
Compound	Observed	Predicted	Pred/Obs	Observed	Predicted	Pred/Obs	Observed	Predicted	Pred/Obs	Observed	Predicted	Pred/Obs
A242N	NA	1.31	NA	NA	1.36	NA						
B222R							1.15	0.89	0.77			
B785F				1.22	1.20	0.98	1.61	1.1	0.68			
B994T				1.18	1.47	1.25	1.57	1.36	0.64			
C213X				1.49	1.54	1.03	1.21	1.9	1.57			
D268Y										1.14	0.92	0.81
D384S				1.93	1.52	0.79	1.16	1.32	1.14			
D863C	0.93	1.07	1.15	1.04	1.10	1.06	1.18	1.11	0.94			
E929K										2.2	1.81	0.82
H938P							0.77	0.92	1.19			
J269A							0.83	1.03	1.24			
K946A	0.99	1.00	1.01				0.80	1.15	1.44	0.98	1.12	1.14
M731N							0.92	1.02	1.11			
N314T	1.07	1.10	1.03	1.16	1.3	1.12	1.13	1.10	0.97			
N314Tm	NA	NA		NA	NA		NA	NA				
N929A				1.39	1.33	0.96	1.56	1.34	0.86			
P662Y							0.69	0.94	1.36			
Q731V	1.09	1.12	1.03	1.10	1.16	1.05	1.25	1.71	1.37			
S537Y							1.41	0.90	0.64			
S961T							0.88	1.01	1.15			
T631W							0.45	1.30	2.89			
T765J				1.07	1.19	1.11	1.07	1.26	1.18			
U924W	1.01	0.94	0.93	0.61	0.58	0.95	0.87	0.51	0.59			
V597G	0.59	0.92	1.56	0.96	1.10	1.15	0.45	1.06	2.22			
Y276D				1.17	1.20	1.03	1.63	1.19	0.73			

C_{max}, maximum plasma drug concentration; ESRD, end-stage renal disease; NA, observed and/or predicted data were not available; Obs, observed; Pred, predicted.

Table 4 Comparison of observed and predicted AUC ratio in hepatic impairment studies

	Mild hepatic impairment			Moderate hepatic impairment			Severe hepatic impairment		
Compound	Observed	Predicted	Pred/Obs	Observed	Predicted	Pred/Obs	Observed	Predicted	Pred/Obs
A242N	1.03	1.92	1.76	1.37	2.78	2.03	1.21	3.40	2.81
B222R				1.03	3.01	2.93			
B785F	0.84	1.36	1.62						
C213X	0.97	1.12	1.16	1.17	1.41	1.21	1.24	1.52	1.23
D268Y				1.66	2.83	1.71	3.87	5.05	1.31
D384S	0.57	1.49	2.60	0.62	3.04	4.87	0.64	4.98	7.81
D863C	1.03	1.58	1.53	1.65	2.88	1.75			
E929K				2.78	5.03	1.81			
H626T	0.78	0.92	1.18	0.80	0.86	1.08	0.61	0.66	1.08
H938P				1.10	1.05	0.95			
J269A				0.99	2.66	2.68			
K946A				2.29	2.23	0.97			
M731N	1.05	1.60	1.52	0.90	2.30	2.57	1.15	3.22	2.80
N314T				1.61	4.57	2.84			
N929A	0.97	1.36	1.40	1.63	1.63	1.00			
P662Y	1.33	1.30	0.98	1.46	2.34	1.60	1.20	2.69	2.24
Q679L				1.79	2.11	1.18			
Q731V	1.02	1.32	1.29	1.31	1.53	1.17	1.35	1.66	1.23
S471Q	0.65	1.24	1.91	1.14	2.45	2.15	0.77	2.82	3.67
S537Y				0.85	1.55	1.82			
S961T	1.15	1.38	1.20	5.61	4.92	0.88			
T535Q	0.98	1.53	1.56	3.04	3.68	1.21	6.82	5.96	0.87
T631W	1.61	1.41	0.89	5.42	2.98	0.55			
U924W	1.20	1.32	1.10	1.10	2.09	1.90	1.80	1.30	0.72
V597G	1.43	1.23	0.86	2.05	1.97	0.96	1.81	2.26	1.25
Y276D	1.17	1.39	1.19						
Y582A	2.65	1.88	0.71	7.96	8.73	1.1	9.47	12.4	1.31

AUC, area under the curve; Obs, observed; Pred, predicted.

impairment across a range of compounds with different clearance and elimination pathways has not been done. As a result, regulatory agencies such as the FDA and the EMA consider the use of PBPK modeling for organ impairment as one of the areas where the confidence in prediction is low.[30,31] This IQ consortium study was conducted specifically to assess the performance of PBPK modeling for predicting exposure changes in the hepatically and renally impaired populations using a large data set, employing a standardized modeling strategy.

The performance of PBPK models for the prediction of exposure changes in organ-impaired populations relies on an accurate representation of the pathophysiological changes in the PBPK platform as well as on the accuracy of pathway characterization in the drug model. Although Simcyp V15 considers most known disease alterations in the organ impaired, some potential alterations such as the CYP inhibition by uremic toxins in RI and changes in hepatic scalars in HI have not been incorporated in Simcyp V15. Reduction in transporter abundance and activity[11] may have to be considered for transporter substrates. For lipophilic compounds that depend on bile solubilization, changes in absorption in hepatic impairment may be important. In addition, it is possible that not all disease alterations in the organ impaired are known today. PBPK models following best practices use clinical data obtained in single and multiple ascending dose studies to verify drug exposure, drug interaction studies to verify metabolism, and mass balance studies to verify clearance pathways. Such models impart confidence to the prediction outcome. In the current analysis, verification of clearance pathways with mass balance data was not always possible, but human mass balance data were available for most compounds (**Tables S7a,b** and **S8a,b**).

Our evaluation identified a tendency to overpredict the effects of hepatic and renal impairments on drug PK. This overprediction is more pronounced with increasing disease severity. No such trends for overprediction or underprediction were obvious in PBPK evaluations reported in the literature (**Table S1a,b**). Plots showing the observed changes in AUC and C_{max} with increasing disease severity (**Figures 4 and 5**), may indicate some evidence for compensatory mechanisms which is more obvious in the case of renal impairment compared with hepatic impairment. Therefore, the current models may need to be revised to

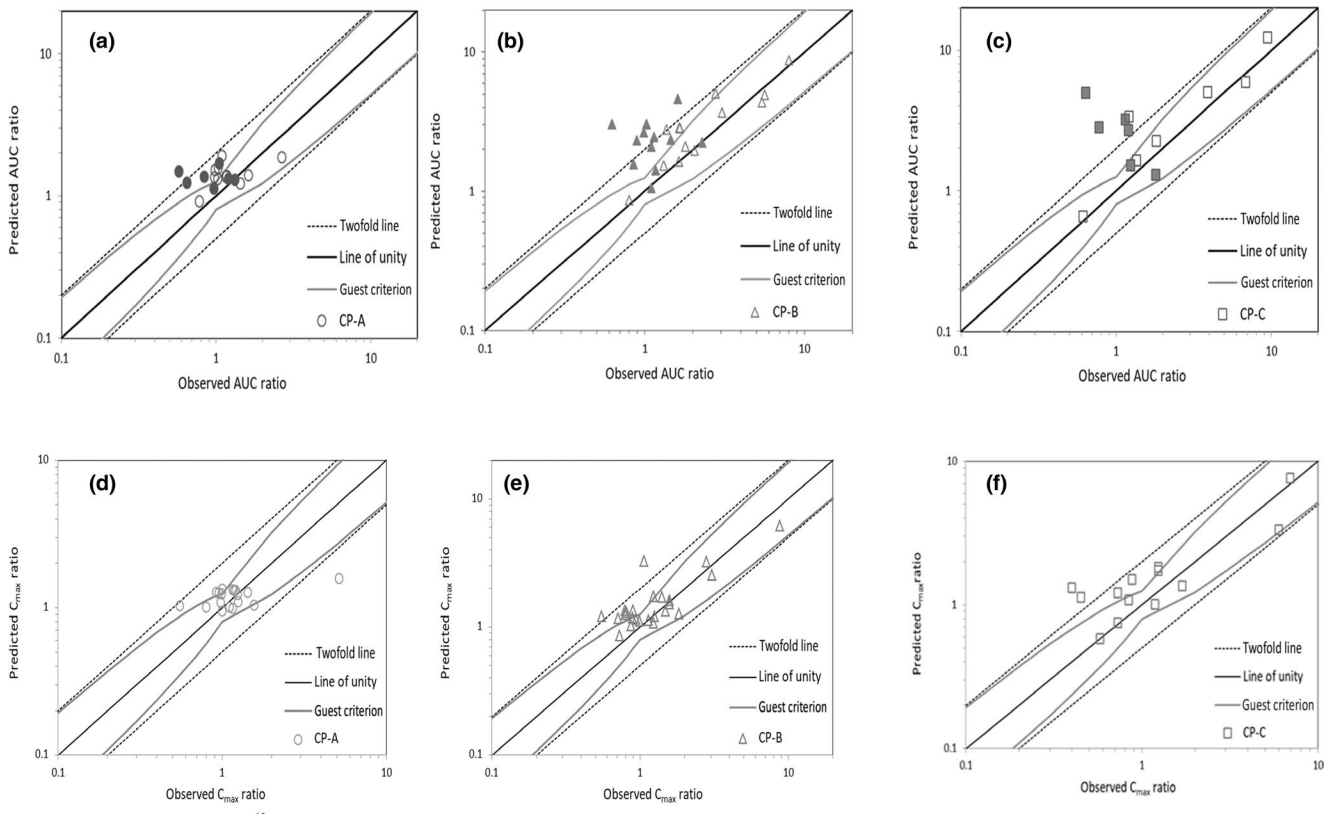

Figure 3 Hepatic Impairment. Comparison of predicted with observed AUC ratios of hepatic impairment patients to matched healthy subjects: (**a**) CP-A (*N* = 18 mild), (**b**) CP-B (*N* = 25 moderate, and (**c**) CP-C (*N* = 13 severe). Closed symbols represent compounds with CL_{iv} < 20 L/h and open symbols represent compounds with CL_{iv} > 20 L/h. Comparison of predicted with observed C_{max} ratios of hepatic impairment patients to matched healthy subjects: (**d**) CP-A (*N* = 18 mild), (**e**) CP-B (*N* = 25 moderate, and (**f**) CP-C (*N* = 13 severe). AUC, area under the curve; CL_{iv}, plasma clearance after intravenous administration of the drug; C_{max}, maximum plasma drug concentration; CP, Child-Pugh classification.

incorporate these compensatory mechanisms when they are better understood. However, given the tendency for PBPK models to overpredict rather than underpredict the effects of impairment for molecules cleared mainly by metabolism, when PBPK predictions of organ-impaired to healthy AUC ratios are within the bioequivalence criteria, even for patients with the highest disease severity, our study suggests that RI and HI clinical studies may not be necessary except for narrow therapeutic index drugs. If a therapeutic index has not been established, PBPK model simulations can help broaden the eligibility criteria in proof-of-concept phase II/III trials and support the inclusion of organ-impaired subjects with or without dose adjustment.

For RI, data from 50 study arms of 25 diverse compounds showed good prediction results with > 90% (47/50) of the AUC ratios of the renally impaired to healthy controls predicted within twofold of the observed ratios. Among the 50 RI study arms, five cases (or 10%) had predicted AUC ratio less than 0.8 which could potentially be concerning in clinical development for narrow therapeutic index drugs (**Table 2**). The results from the current study for mild and moderate impairment are generally in good agreement with the prediction successes reported in the literature (**Table S1a**).[32] They serve to enhance the confidence in applying PBPK modeling to predict changes in exposure in the renally impaired population for compounds with a wide safety margin, supported by a totality of evidence from mass balance, absolute bioavailability, DDI and hepatic impairment studies.

A dedicated renal impairment study for drugs that are predominantly eliminated by the kidney and likely to be used by patients with kidney impairment should include ESRD subjects. These subjects are difficult to recruit given their limited numbers. Only a small fraction of this patient group may consider participating in a PK study, since ESRD patients experience significant mortality, morbidity, and a reduced quality of life. A smaller subset of those willing to participate will qualify based on the medical history, complications due to disease, concomitant medications, or other screening criteria. Dosing ESRD patients with a nonapproved drug may pose a safety risk. Therefore, regulatory agencies and institutional review boards require that adequate safety measures are in place for enrolling these subjects in late-stage phase II/III clinical trials. Given these challenges to conducting renal impairment studies, PBPK predictions verified for mildly and moderately impaired populations can be used to supplement clinical data in the severely impaired and ESRD patients. Since the model predictions tended to overestimate rather than underpredict the risk in severely impaired and ERSD patients, the predicted risk for these two classes is likely to be a worst-case scenario.

Among compounds that were studied clinically in more than one category of hepatic impairment population, when the effects of moderate hepatic impairment were predicted within twofold of clinically observed values, the effects of mild and/or severe hepatic impairment were also generally predicted within twofold regardless of their clearance (**Table S8a,b**). This finding supports

Table 5 Comparison of observed and predicted C_{max} ratio in hepatic impairment studies

	Mild hepatic impairment			Moderate hepatic impairment			Severe hepatic impairment		
Compound	Observed	Predicted	Pred/Obs	Observed	Predicted	Pred/Obs	Observed	Predicted	Pred/Obs
A242N	1.18	1.30	1.10	1.58	1.51	0.96	1.24	1.73	1.40
B222R				0.94	1.14	1.21			
B785F	0.95	1.24	1.31						
C213X	1.16	1.31	1.13	1.23	1.72	1.40	1.24	1.83	1.48
D268Y				0.81	1.28	1.58	0.88	1.5	1.70
D384S	0.55	1.02	1.85	0.55	1.19	2.16	0.45	1.13	2.51
D863C	0.99	1.23	1.24	1.49	1.32	0.89			
E929K				1.06	3.23	3.05			
H626T	1.00	0.94	0.94	0.73	0.85	1.16	0.73	0.75	1.03
H938P				0.99	1.10	1.11			
J269A				0.90	1.34	1.49			
K946A				NA	NA				
M731N	1.16	0.98	0.84	0.87	1.01	1.16	0.84	1.08	1.29
N314T				1.41	1.70	1.21			
N929A	1.00	1.33	1.33	1.58	1.60	1.01			
P662Y	1.11	1.00	0.90	0.89	1.17	1.31	0.73	1.21	1.66
Q679L				1.25	1.19	0.95			
Q731V	1.25	1.09	0.87	1.14	1.11	0.97	1.19	1.01	0.85
S471Q	0.80	1.00	1.25	0.79	1.24	1.57	0.40	1.32	3.30
S537Y				0.71	1.16	1.63			
S961T	1.21	1.30	1.04	2.81	3.18	1.13			
T535Q	0.92	1.26	1.37	3.06	2.52	0.82	5.97	3.34	0.56
T631W	1.43	1.26	0.88	1.23	1.06	0.86			
U924W	0.98	1.08	1.10	0.79	1.34	1.7	0.58	0.58	1.00
V597G	1.57	1.03	0.66	1.83	1.26	0.69	1.69	1.35	0.80
Y276D	1.24	1.22	0.98						
Y582A	5.16	1.57	0.30	8.76	6.13	0.70	6.96	7.62	1.09

C_{max}, maximum plasma drug concentration; NA, observed and/or predicted data were not available.

the use of PBPK predictions for supplementing clinical data, once the model is verified in one class of a hepatically impaired population. However, an extrapolation of prediction results to patient groups that were difficult to recruit can only be done if the metabolic and disposition characteristics as well as PK variability of the compound in question are well represented in the drug model and the disease modification of these processes with the extent of organ impairment is captured in the physiological model.

In our analyses, the cirrhotic population models resulted in predicted hepatic impaired to healthy AUC ratios of > 1. However, the observed AUC ratios ranged from < 1 to ~ 10 (**Table 4**). A reduced rate of bile acid output or lower bile acid concentration leading to a reduced drug absorption in hepatic impairment could explain a < 1 observed AUC ratio.[33,34] These pathophysiological changes in the hepatic impaired were not considered in the model.

The compounds in our study had very little transporter activity. In the literature however, a PBPK fitting approach has been described for five liver transporter substrates to understand the impact of cirrhosis on the transporter activity in CP-A and CP-B groups.[29] The analysis assumed that all uptake transporters were similarly affected in the disease populations. In another study, decreases in CYP3A4 activities were observed and characterized in subjects with nonalcoholic fatty liver (NAFL) and with nonalcoholic steatohepatitis (NASH), since NAFL may lead to NASH and is one of the major causes of chronic liver diseases. Incorporation of the changes in the CYP3A4 activities and protein expression in the PBPK model of midazolam enabled the use of a PBPK model for the prediction of the changes in midazolam PK in patients with NAFL and NASH.[35]

Compared with renal impairment, fewer successful PBPK predictions have been reported in the literature for hepatic impairment (**Table S1b**). The disposition of simeprevir in humans is characterized by hepatic uptake by organic anion transporting polypeptide 1B1/3 (OATP1B1/3) and metabolism by CYP3A4. PBPK simulations of various drug–drug interactions[31] could explain the observed nonlinear PK of simeprevir at therapeutic doses as due to saturation of CYP3A4-mediated gut and liver metabolism and hepatic uptake. Using the mild hepatic impairment population as a surrogate, exposure changes of simeprevir in HCV-infected White subjects were predicted well.[32]

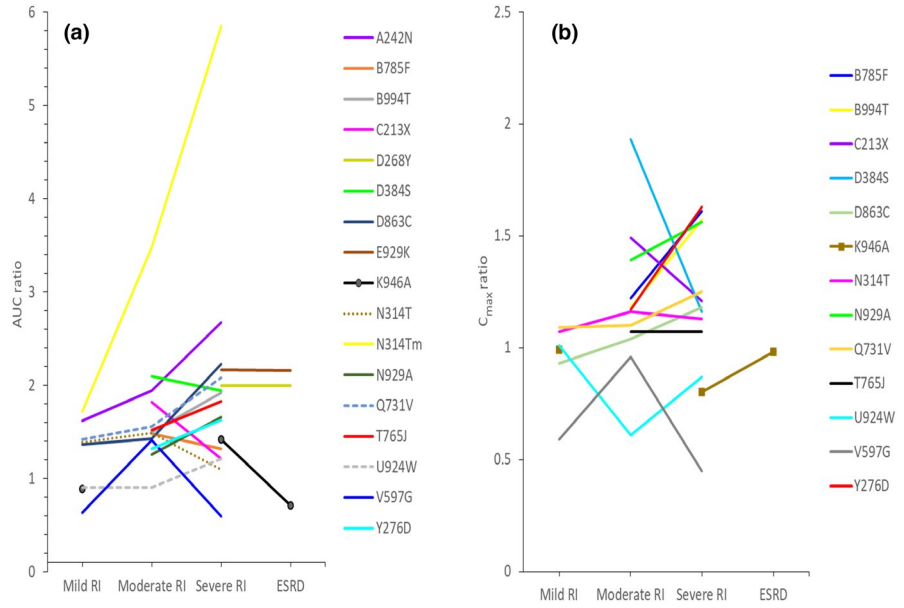

Figure 4 Observed (**a**) AUC ratios and (**b**) C_{max} ratios of renal impairment patients to healthy subjects for compounds that were studied in two or more impairment categories. AUC, area under the curve; C_{max}, maximum plasma drug concentration.

The application of modeling strategy proposed by Kuemmel[2] for the prediction of PK in hepatic impairment is illustrated by two examples (**Tables S6**, **S9** and **S10**).

PERSPECTIVE AND FUTURE DIRECTION

A unique data set comprising 106 hepatic and renal impairment clinical study arms with 30 compounds compiled from 19 IQ Consortium member companies was employed to evaluate the performance of PBPK models to predict drug exposure in organ-impaired populations. PBPK predictions of exposure in the renally and hepatically impaired populations were within twofold of the observed data in > 90% and > 70% of the studies, respectively. For renal impairment the accuracy of the predictions was less than twofold, especially for compounds for which renal clearance contributed significantly to their elimination (renal excretion > 25%, indicating up to 75% metabolism). Cases outside the twofold limit tended to be overpredicted rather than underpredicted for both populations and belonged to groups with high disease severity. The explanation could lie in compensatory mechanisms such as cardiovascular changes and acid–base

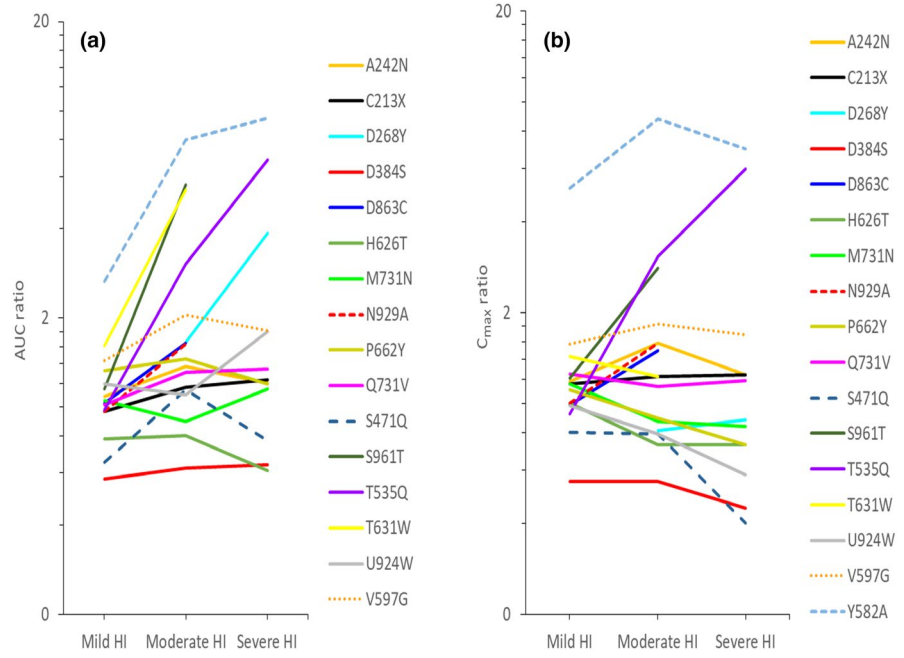

Figure 5 Observed (**a**) AUC ratios and (**b**) C_{max} ratios of hepatic impairment patients to healthy subjects for compounds that were studied in two or more impairment categories.

imbalance that may become important with increasing disease severity[36,37] but were not captured in the model. A few remaining knowledge gaps in the pathophysiological changes in RI and HI have to be filled and sources of variability understood to further improve exposure predictions in the organ-impaired populations.

Findings from our study suggest that a verified and robust PBPK model may be applied with confidence to supplement missing clinical data in hepatic and renal impairment subjects when recruitment is incomplete in one or more categories of organ impairment. Given the tendency for PBPK models to overpredict rather than underpredict, when PBPK predictions of organ-impaired to healthy AUC ratios are within the bioequivalence criteria, our study supports restricting the renal and hepatic impairment studies to narrow therapeutic index drugs. Confirmatory studies for narrow therapeutic index drugs may be performed with a lean design in severe impairment subjects and the outcome used to support the label. Such confirmatory studies may be considered later in phase III rather than in phase II. In the absence of information on the therapeutic index of a drug, modeling results may be used to support inclusion of organ-impaired subjects with less disease severity in phase II/III trials.

When PBPK predictions of AUC ratios are outside the bioequivalence limits, model predictions can be used to design hepatic and renal impairment studies and to decide on the timing of these studies. PBPK modeling can contribute to a totality of evidence to supplement limited observations in clinical studies.

SUPPORTING INFORMATION

Supplementary information accompanies this paper on the *Clinical Pharmacology & Therapeutics* website (www.cpt-journal.com).

ACKNOWLEDGMENTS

The authors wish to thank Fang Ma (Genentech), Wen Lin (Novartis), Jin Chen (Novartis), Heidi Einolf (Novartis), Felix Huth (Novartis), Imad Hanna (Novartis), Handan He (Novartis), Avantika Barve (Novartis), Loeckie De Zwart (Janssen), Hugh Barton (Pfizer), Jeanine Ballard (Merck), Tamara Cabalu (Merck) for their contribution to the data collection, model development and simulation, and scientific discussions.

FUNDING

No funding was received for this work.

CONFLICT OF INTEREST

The authors declared no competing interests for this work. All authors' places of employment are listed on the title page.

1. Poggesi, I., Snoeys, J. & Van Peer, A. The successes and failures of physiologically based pharmacokinetic modeling: there is room for improvement. *Expert Opin. Drug Metab. Toxicol.* **10**, 631–635 (2014).
2. Kuemmel, C. *et al*. Consideration of a credibility assessment framework in model-informed drug development: potential application to physiologically-based pharmacokinetic modeling and simulation. *CPT: Pharmacometrics Syst. Pharmacol.* **9**, 21–28 (2020).
3. Shebley, M. *et al*. Physiologically based pharmacokinetic model qualification and reporting procedures for regulatory submissions: a consortium perspective. *Clin. Pharmacol. Ther.* **104**, 88–110 (2018).
4. Jones, H.M. *et al*. Physiologically based pharmacokinetic modeling in drug discovery and development: a pharmaceutical industry perspective. *Clin. Pharmacol. Ther.* **97**, 247–262 (2015).
5. Mehrotra, N. *et al*. Role of quantitative clinical pharmacology in pediatric approval and labeling. *Drug Metab. Dispos.* **44**, 924–933 (2016).
6. Grimstein, M. *et al*. Physiologically based pharmacokinetic modeling in regulatory science: an update from the U.S. Food and Drug Administration's office of clinical pharmacology. *J. Pharm. Sci.* **108**, 21–25 (2019).
7. Luzon, E., Blake, K., Cole, S., Nordmark, A., Versantvoort, C. & Berglund, E.G. Physiologically based pharmacokinetic modeling in regulatory decision-making at the European Medicines Agency. *Clin. Pharmacol. Ther.* **102**, 98–105 (2017).
8. Sato, M. *et al*. Quantitative modeling and simulation in PMDA: a Japanese regulatory perspective. *CPT Pharmacometrics Syst. Pharmacol.* **6**, 413–415 (2017).
9. Yeung, C.K., Shen, D.D., Thummel, K.E. & Himmelfarb, J. Effects of chronic kidney disease and uremia on hepatic drug metabolism and transport. *Kidney Int.* **85**, 522–528 (2014).
10. Wu, W., Bush, K.T. & Nigam, S.K. Key role for the organic anion transporters, OAT1 and OAT3, in the *in vivo* handling of uremic toxins and solutes. *Sci. Rep.* **7**, 4939 (2017).
11. Drozdzik, M. *et al*. Protein abundance of hepatic drug transporters in patients with different forms of liver damage. *Clin. Pharmacol. Ther.* **107**, 1138–1148 (2020).
12. McConn, D.J. 2nd *et al*. Reduced duodenal cytochrome P450 3A protein expression and catalytic activity in patients with cirrhosis. *Clin. Pharmacol. Ther.* **85**, 387–393 (2009).
13. Bayraktar, U.-D., Seren, S. & Bayraktar, Y. Hepatic venous outflow obstruction: three similar syndromes. *World J. Gastroenterol.* **13**, 1912–1927 (2007).
14. Dessouky, B.A.M., El Abd, O.L. & Abdel Aal, E.S.M. Intrahepatic vascular shunts: strategy for early diagnosis, evaluation and management. *Egyptian J. Radiol. Nucl. Med.* **42**, 19–34 (2011).
15. Ghibellini, G., Leslie, E.M. & Brouwer, K.L.R. Methods to evaluate biliary excretion of drugs in humans: an updated review. *Mol. Pharm.* **3**, 198–211 (2006).
16. US Food and Drug Administration. Guidance for industry: pharmacokinetics in patients with impaired renal function — study design, data analysis, and impact on dosing and labeling <https://www.fda.gov/regulatory-information/search-fda-guidance-documents/pharmacokinetics-patients-impaired-renal-function-study-design-data-analysis-and-impact-dosing-and> (September 2020).
17. US Food and Drug Administration. Guidance for industry: pharmacokinetics in patients with impaired hepatic function: study design, data analysis, and impact on dosing and labeling <https://www.fda.gov/media/71311/download> (May 2003).
18. US Food and Drug Administration. Draft guidance: pharmacokinetics in patients with impaired renal function — study design, data analysis, and impact on dosing and labeling <https://www.fda.gov/regulatory-information/search-fda-guidance-documents/pharmacokinetics-patients-impaired-renal-function-study-design-data-analysis-and-impact-dosing-and> (September 2020).
19. European Medicines Agency. Guideline on the evaluation of the pharmacokinetics of medicinal products in patients with impaired hepatic function <https://www.ema.europa.eu/en/documents/scientific-guideline/guideline-evaluation-pharmacokinetics-medicinal-products-patients-impaired-hepatic-function_en.pdf> (February 2005).
20. Durand, F. & Valla, D. Assessment of the prognosis of cirrhosis: Child-Pugh versus MELD. *J. Hepatol.* **42**, S100–S107 (2005).

21. Talal, A.H., Venuto, C.S. & Younis, I. Assessment of hepatic impairment and implications for pharmacokinetics of substance use treatment. *Clin. Pharmacol. Drug Dev.* **6**, 206–212 (2017).
22. Xiao, J.J., Chen, J.S., Lum, B.L. & Graham, R.A. A survey of renal impairment pharmacokinetic studies for new oncology drug approvals in the USA from 2010 to early 2015: a focus on development strategies and future directions. *Anticancer Drugs* **28**, 677–701 (2017).
23. D'Cunha, R. & Lin, S. A review of regulatory guidance for conducting hepatic impairment studies: a case study in oncology. *J. Oncol. Cancer Res.* **2**, 14–22 (2018).
24. Johnson, T.N., Boussery, K., Rowland-Yeo, K., Tucker, G.T. & Rostami-Hodjegan, A. A semi-mechanistic model to predict the effects of liver cirrhosis on drug clearance. *Clin. Pharmacokinet.* **49**, 189–206 (2010).
25. Rowland Yeo, K., Aarabi, M., Jamei, M. & Rostami-Hodjegan, A. Modeling and predicting drug pharmacokinetics in patients with renal impairment. *Expert Rev. Clin. Pharmacol.* **4**, 261–274 (2011).
26. Heimbach, T. *et al*. Physiologically based pharmacokinetic modeling to supplement Nilotinib pharmacokinetics and confirm dose selection in pediatric patients. *J. Pharm. Sci.* **108**, 2191–2198 (2019).
27. Follman, K.E. & Morris, M.E. Simulation-based analysis of the impact of renal impairment on the pharmacokinetics of highly metabolized compounds. *Pharmaceutics* **11**, 105 (2019).
28. Tan, M.-L. *et al*. Use of physiologically based pharmacokinetic modeling to evaluate the effect of chronic kidney disease on the disposition of hepatic CYP2C8 and OATP1B drug substrates. *Clin. Pharmacol. Ther.* **105**, 719–729 (2019).
29. Guest, E.J., Aarons, L., Houston, J.B., Rostami-Hodjegan, A. & Galetin, A. Critique of the two-fold measure of prediction success for ratios: application for the assessment of drug–drug interactions. *Drug Metab. Dispos.* **39**, 170–173 (2011).
30. Wagner, C. *et al*. Application of Physiologically Based Pharmacokinetic (PBPK) modeling to support dose selection: report of an FDA public workshop on PBPK. *CPT: Pharmacometrics Syst. Pharmacol.* **4**, 226–230 (2015).
31. Shepard, T., Scott, G., Cole, S., Nordmark, A. & Bouzom, F. Physiologically based models in regulatory submissions: output from the ABPI/MHRA forum on physiologically based modeling and simulation. *CPT: Pharmacometrics Syst. Pharmacol.* **4**, 221–225 (2015).
32. Hsueh, C.-H., Hsu, V., Zhao, P., Zhang, L., Giacomini, K.M. & Huang, S.-M. PBPK modeling of the effect of reduced kidney function on the pharmacokinetics of drugs excreted renally by organic anion transporters. *Clin. Pharmacol. Ther.* **103**, 485–492 (2018).
33. Horsmans, Y. *et al*. Effects of mild to severe hepatic impairment on the pharmacokinetics of Sonidegib: a multicenter, open-label. Parallel-Group Study. *Clin. Pharmacokinet.* **57**, 345–354 (2018).
34. Ouwerkerk-Mahadevan, S. *et al*. Pharmacokinetics of bound and unbound telaprevir in cirrhotic patients with moderate and severe hepatic impairment. *J. Clin. Pharmacol.* **55**, 1147–1156 (2015).
35. Jamwal, R., de la Monte, S.M., Ogasawara, K., Adusumalli, S., Barlock, B.B. & Akhlaghi, F. Nonalcoholic fatty liver disease and diabetes are associated with decreased CYP3A4 protein expression and activity in human liver. *Mol. Pharm.* **15**, 2621–2632 (2018).
36. Fede, G., Privitera, G., Tomaselli, T., Spadaro, L. & Purrello, F. Cardiovascular dysfunction in patients with liver cirrhosis. *Ann. Gastroenterol.* **28**, 31–40 (2015).
37. Scheiner, B. *et al*. Acid-base disorders in liver disease. *J. Hepatol.* **67**, 1062–1073 (2017).